Ferromagnetic Sc-doped AlN sixfold-symmetrical hierarchical nanostructures

W. W. Lei, D. Liu, P. W. Zhu, X. H. Chen, Q. Zhao et al.

Related Articles

Design of remnant magnetization FeCoV films as compact, heatless neutron spin rotators
Appl. Phys. Lett. 101, 182404 (2012)

Sub-micron mapping of GHz magnetic susceptibility using scanning transmission x-ray microscopy
Appl. Phys. Lett. 101, 182407 (2012)

Structural, magnetic, and optical properties of Pr and Zr codoped BiFeO3 multiferroic ceramics
J. Appl. Phys. 112, 094102 (2012)

Controlling the current flux in magnetic-barrier induced graphene waveguide
Appl. Phys. Lett. 101, 163104 (2012)

Hard magnetic properties of Mn-Ga melt-spun ribbons
J. Appl. Phys. 112, 083901 (2012)

Additional information on Appl. Phys. Lett.

Journal Homepage: http://apl.aip.org/

Journal Information: http://apl.aip.org/about/about_the_journal

Top downloads: http://apl.aip.org/features/most_downloaded

Information for Authors: http://apl.aip.org/authors

Ferromagnetic Sc-doped AlN sixfold-symmetrical hierarchical nanostructures

W. W. Lei, D. Liu, P. W. Zhu, X. H. Chen, Q. Zhao, G. H. Wen, Q. L. Cui,[a)] and G. T. Zou
State Key Laboratory of Superhard Materials, Jilin University, Changchun 130012, People's Republic of China

Sc-doped AlN (AlN:Sc) sixfold-symmetrical hierarchical nanostructures were grown by direct current (dc) arc discharge plasma method using the direct reaction of Al and Sc metals with N_2 gas. Energy-dispersive x-ray spectroscopy, x-ray diffractometry, and Raman spectra analysis clearly showed that Sc was doped in the AlN hierarchical nanostructures. The magnetization curves indicate the existence of room-temperature ferromagnetic behavior. The saturation magnetization and the coercive fields (H_c) of the AlN:Sc nanostructures are about 0.04 emu g^{-1} and 200 Oe, respectively. The results reveal that Sc is a potential nonmagnetic dopant for preparing diluted magnetic semiconductor nanomaterials. © *2009 American Institute of Physics.* [doi:10.1063/1.3248257]

Recently, diluted magnetic semiconductors (DMSs) have attracted a great deal of attention because of their potential applications in the field of spin-dependent semiconductor electronics.[1,2] It is well known that the most primary method is the introducing appropriate rare-earth dopants or transition metals (TMs) into a semiconductor to produce a DMS, as they can often induce dramatic changes in the optical, electrical, and magnetic properties.[3,4] Besides the well studied II-VI and III-V DMS, doping of III nitrides with different rare-earth elements or TMs has gained a lot of attention not only because of its importance in optoelectronics but also due to its potential as a promising material for spintronics.[5,6] Although many efforts have been made to explore the synthesis and magnetic properties of AlN-based DMS bulk materials and films,[7–10] there are very few research groups reported the synthesis of nanostructures.[11,12] Especially hierarchical structured nanomaterials, which have dual or multiple morphologies and structures, have attracted increasing interest because of their structural complexity and greater functionality.[13,14] Recently, Bai[15] indicated that cubic ScN is a good lattice match for zinc blende III-A nitrides. Therefore combining the two binary semiconductors to form $Sc_xAl_{1-x}N$ alloys could be useful in technological applications.[16] However, the magnetism of the nitride alloys has not yet been reported. Until now, no work on synthesis of Sc-doped AlN sixfold-symmetrical hierarchical nanostructures was presented. Here we investigated the synthesis of Sc-doped AlN sixfold-symmetrical hierarchical nanostructures without introducing any catalysts and templates. Their structural and magnetic properties are characterized.

The AlN:Sc sixfold-symmetrical hierarchical nanostructures were synthesized in an improved dc arc discharge plasma setup.[17] In a typical run, aluminum (purity 99.99%) powders, scandium (purity 99.99%) powders and N_2 gas (purity 99.99%) were used as sources. The chamber pressure was evacuated to less than 1 Pa, and then working gas was introduced into the chamber. The N_2 pressure is at 30 kPa. The input current was maintained at 120 A and the voltage was a little higher than 20 V. After growth for 20 min, a layer of gray-colored flocky product was deposited on the W cath-

ode. The crystal structures of the product were characterized by x-ray diffractometry (XRD) (Rigaku D/Max-A, Cu $K\alpha$). The chemical composition of the product was determined by energy-dispersive x-ray spectroscopy (EDS). The morphology and structure were characterized by field-emission scanning electron microscopy (SEM) XL 30 ESEM FEG) and high-resolution transmission electron microscopy (HRTEM) JEM-2100F. Micro-Raman spectroscopy was measured by Renishaw inVia (excited with an Ar$^+$ line at 514 nm). The magnetic properties were measured using a vibrating sample magnetometer at room temperature.

Figure 1 displays the powder XRD patterns of the undoped AlN and Sc-doped AlN sixfold-symmetrical hierarchical nanostructures. All observed peaks can be readily indexed to pure hexagonal phase [space group: $P6_3mc$ (186)] of AlN.[18] No peaks of any other phases or impurities were
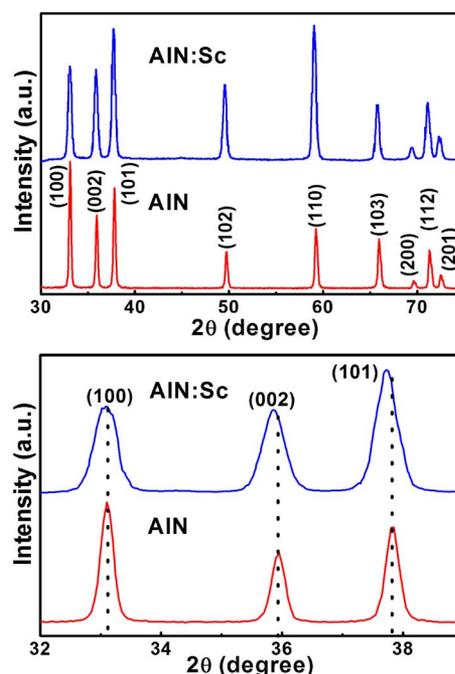

FIG. 1. (Color online) (a) XRD patterns of AlN and AlN:Sc hierarchical nanostructures. (b) The enlarged (100), (002), and (101) peaks.
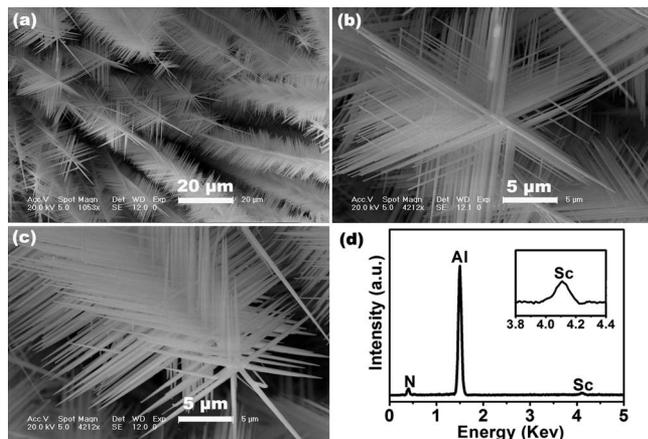
a)Electronic mail: cql@jlu.edu.cn.

FIG. 2. (a) A low magnification SEM image of the as-synthesized AlN:Sc sixfold-symmetrical hierarchical nanostructures. (b) A typical front view of the sixfold-symmetrical hierarchical nanostructure. (c) A side view of a single sixfold-symmetrical hierarchical nanostructure. (d) EDS spectrum of the as-synthesized AlN:Sc sixfold-symmetrical hierarchical nanostructures.

FIG. 4. (Color online) Typical Raman spectra of AlN and AlN:Sc sixfold-symmetrical hierarchical nanostructures.

detected. The (100), (002), and (101) peaks positions of the AlN:Sc are slightly shifted to lower angles compared with AlN hierarchical nanostructures [see the Fig. 1(b)], suggesting the increase of the lattice constants due to the effective substitution of larger radius Sc^{3+} ions ($r_{Sc}=0.73$ Å) for the Al^{3+} ions ($r_{Al}=0.51$ Å), as reported in Mn-doped ZnO nanowires.[19]

Typical SEM images of the as-synthesized product are shown in Fig. 2. Figure 2(a) shows a low-magnification image of the as-synthesized product. They reveal a clear and well-defined sixfold-symmetrical structure with a "backbone" surrounded by radial oriented "nanowires." Typical backbone has a length range of several tens of microns and a width of about 1.5 μm. The nanowires are typically about 10 μm in length and 200–500 nm in diameter. A typical front view of the nanostructure indicates a sixfold-symmetrical ordered assembly [Fig. 2(b)]. The distribution of the nanowires around the backbone has an angle interval of 60°. Figure 2(c) is a side view of a single sixfold-symmetrical nanostructure at higher magnification. The nanowires grow in a single row. The chemical composition of AlN:Sc sixfold-symmetrical hierarchical nanostructures was determined from EDS spectrum [Fig. 2(d)]. Quantitative analysis reveals that the atomic ratio of Al:N:Sc is about 52.36:46.25:1.39.

The crystalline structure of AlN sixfold-symmetrical nanostructure was also studied by TEM. Figure 3(a) is a
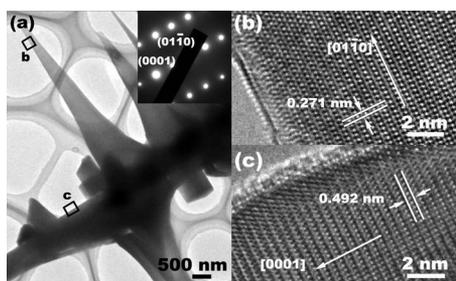

FIG. 3. (a) TEM image of the AlN:Sc sixfold-symmetrical hierarchical nanostructure. Inset presents its corresponding electron diffraction pattern. (b) and (c) are HRTEM images taken from the tip of the nanowire and the backbone of the AlN:Sc sixfold-symmetrical hierarchical nanostructure.
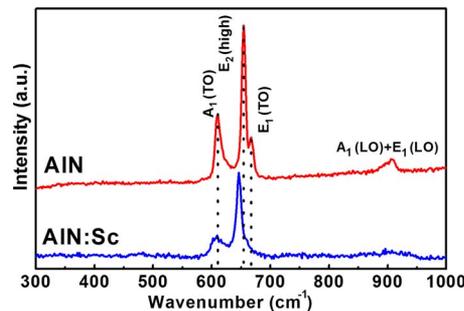
typical TEM image of the nanowires-backbone junction structures. The nanowires vertically grow out from the backbone. The SAED pattern [inserted Fig. 3(a)] is consistent with the hexagonal wurtzite structure of AlN with no second phase detected. Figures 3(b) and 3(c) are HRTEM images taken from the tip of the nanowire and the backbone [from the square boxes in Fig. 3(a)], respectively. The backbone axis is along the [0001] direction, whereas the nanowires axis is along the [01$\bar{1}$0] direction, with lattice spacings determined to be 0.492 and 0.271 nm, respectively. They correspond to (0001) and (01$\bar{1}$0) crystal planes, respectively. Both HRTEM and selected area electron diffraction (SAED) images indicate that the growth direction of the backbone is [0001], and the nanowires are [01$\bar{1}$0] (and equivalent directions).

The Raman spectra of the undoped AlN and Sc doped AlN sixfold-symmetrical hierarchical nanostructures were obtained at room temperature. As shown in Fig. 4, three distinct peaks centered at 611.4, 654.3, and 665.9 cm^{-1} are correlated with the first-order vibrational modes of $A_1(TO)$, $E_2(high)$, and $E_1(TO)$ for undoped AlN hierarchical nanostructures, respectively. The low-intensity broad peak around 903.8 cm^{-1} is assigned to the overlap of the modes $A_1(LO)$ and $E_1(LO)$. It is worth noting the slight redshift of $E_2(high)$, $A_1(TO)$, and $E_1(TO)$ of the AlN:Sc sixfold-symmetrical hierarchical nanostructures relative to those of the undoped AlN hierarchical nanostructures, which may be attributed to the disorder of the crystals due to the incorporation of Sc. This further indicates that the Al cation (Al^{3+}) have been substituted with Sc cation (Sc^{3+}), which is consistent with the results of XRD. These results are in good agreement with the results for AlN:Cu nanorods.[12]

We suggest that the vapor-solid (VS) mechanism might dominate the growth of the present unusual structures because no metal nanoparticles were found on the tips of the nanowires. The growth of the structure presented in the present study can be separated into two stages. The first stage is a fast growth of AlN:Sc backbone along the [0001] growth direction because there are enough Al, Sc and N during initial stages in the high N_2 pressure. The one-dimensional AlN:Sc crystals grow along the [0001] direction is attributed to the intrinsic properties of AlN.[20] The second stage is the nucleation and epitaxial growth of the AlN:Sc branches on the backbone. This stage is slower than the first stage because the branches are uniform and much shorter in length. In this stage, the growth of AlN:Sc branches along the six growth directions: $\pm[10\bar{1}0]$, $\pm[01\bar{1}0]$, and $\pm[\bar{1}100]$ and the
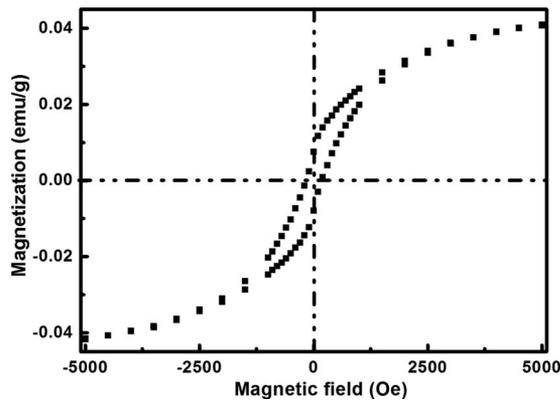
FIG. 5. Magnetization hysteresis loop of the AlN:Sc sixfold-symmetrical hierarchical nanostructures measured at room temperature.

angles between the growth directions of the two adjacent branches is 60°. Finally, the AlN:Sc sixfold-symmetrical hierarchical nanostructures were obtained on the W cathode. Similar growth mechanisms are reported in the literature for ZnO nanowire-nanoribbon junction arrays.[13]

Magnetic properties of the AlN:Sc sixfold-symmetrical hierarchical nanostructures were measured at 300 K, and the results are presented in Fig. 5. Hysteresis loop can be observed, showing obvious ferromagnetic characteristics at room temperature. The saturation magnetization and the coercive fields (H_c) of the AlN:Sc are about 0.04 emu g^{-1} and 200 Oe, respectively. According to our results of XRD, HR-TEM, and Raman spectra, the possibility of Sc metal and secondary phases such as ScN and ScAl can be ruled out. Since neither Al^{3+} nor Sc^{3+} are magnetic ions, so the observation of ferromagnetism is intrinsic properties in AlN:Sc. Recently, Venkatesan *et al.*[21] have reported the room-temperature ferromagnetism is observed in Sc-doped ZnO films. They suggested a source of magnetism, namely, triplet states associated with two-electron defects. On this basis, it can be concluded that in our AlN:Sc nanostructures, the likely origin of the triplet states is Sc^{+3} introduced Al vacancies which is similar to that of the Sc^{+3} introduced Zn vacancies in Sc-doped ZnO films. It has been reported that the Al vacancies have a triplet ground state.[22] A recent calculation by Wu *et al.*[23] for AlN indicates that the Al vacancies in AlN favors a spin-polarized state with total magnetic moment $3.0\mu_B$. Similar ferromagnetism due to create cation vacancies was also predicted for Hf vacancies in HfO_2 and Ca vacancies in CaO using *ab initio* calculation.[24,25] Therefore, the observation of ferromagnetism in the AlN:Sc nanostructures may be due to the Sc^{+3} introduced Al vacancies. Further investigations on the origin of the observed magnetic behavior of AlN:Sc nanostructures is currently in progress.

In summary, we reported on the fabrication of Sc-doped AlN sixfold-symmetrical hierarchical nanostructures showing ferromagnetic behavior a room temperature using dc arc discharge plasma method. This synthetic success indicates that Sc is a potential nonmagnetic dopant. The synthesis approach provides an opportunity for preparing nanostructures of DMS.

[1] P. Sharma, A. Gupta, K. V. Rao, F. J. Owens, R. Sharmaa, R. Ahuja, J. M. O. Guillen, B. Johansson, and G. A. Gehring, Nature Mater. **2**, 673 (2003).
[2] H. Ohno, Science **281**, 951 (1998).
[3] J. J. Liu, M. H. Yu, and W. L. Zhoua, Appl. Phys. Lett. **87**, 172505 (2005).
[4] D. S. Han, J. Park, K. W. Rhie, S. Kim, and J. Chang, Appl. Phys. Lett. **86**, 032506 (2005).
[5] H. Ohno, A. Shen, F. Matsukura, A. Oiwa, A. Endo, S. Katsumoto, and Y. Iye, Appl. Phys. Lett. **69**, 363 (1996).
[6] M. L. Reed, N. A. El-Masry, H. H. Stadelmaier, M. K. Ritums, M. J. Reed, C. A. Parker, J. C. Roberts, and S. M. Bedair, Appl. Phys. Lett. **79**, 3473 (2001).
[7] S. Y. Han, J. Hite, G. T. Thaler, R. M. Frazier, C. R. Abernathy, S. J. Pearton, H. K. Choi, W. O. Lee, Y. D. Park, J. M. Zavada, and R. Gwilliam, Appl. Phys. Lett. **88**, 042102 (2006).
[8] D. Kumar, J. Antifakos, M. G. Blamire, and Z. H. Barber, Appl. Phys. Lett. **84**, 5004 (2004).
[9] S. G. Yang, A. B. Pakhomov, S. T. Hung, and C. Y. Wong, Appl. Phys. Lett. **81**, 2418 (2002).
[10] S. Y. Wu, H. X. Liu, L. Gu, R. K. Singh, L. Budd, M. Schilfgaarde, W. R. McCartney, D. J. Smith, and N. Newman, Appl. Phys. Lett. **82**, 3047 (2003).
[11] X. H. Ji, S. P. Lau, S. F. Yu, H. Y. Yang, T. S. Herng, A. Sedhain, J. Y. Lin, H. X. Jiang, K. S. Teng, and J. S. Chen, Appl. Phys. Lett. **90**, 193118 (2007).
[12] X. H. Ji, S. P. Lau, S. F. Yu, H. Y. Yang, T. S. Herng, and J. S. Chen, Nanotechnology **18**, 105601 (2007).
[13] P. Gao and Z. L. Wang, J. Phys. Chem. B **106**, 12653 (2002).
[14] Y. B. Tang, H. T. Cong, Z. M. Wang, and H.-M. Cheng, Appl. Phys. Lett. **89**, 253112 (2006).
[15] X. Bai, Ph.D. thesis, Ohio University, 2000.
[16] M. Akiyama, T. Kamohara, K. Kano, A. Teshigahara, Y. Takeuchi, and N. Kawahara, Adv. Mater. **21**, 593 (2009).
[17] W. W. Lei, D. Liu, J. Zhang, B. B. Liu, P. W. Zhu, T. Cui, Q. L. Cui, and G. T. Zou, Chem. Commun. (Cambridge) **2009**, 1365.
[18] JCPDS Card No. 08–0262.
[19] Y. J. Kang, D. S. Kim, S. H. Lee, J. Park, J. Chang, J. Y. Moon, G. Lee, J. Yoon, Y. Jo, and M.-H. Jung, J. Phys. Chem. C **111**, 14956 (2007).
[20] W. W. Lei, D. Liu, P. W. Zhu, Q. S. Wang, G. Liang, J. Hao, X. H. Chen, Q. L. Cui, and G. T. Zou, J. Phys. Chem. C **112**, 13353 (2008).
[21] M. Venkatesan, C. B. Fitzgerald, J. G. Lunney, and J. M. D. Coey, Phys. Rev. Lett. **93**, 177206 (2004).
[22] C. Stampfl and C. G. Van de Walle, Phys. Rev. B **65**, 155212 (2002).
[23] R. Q. Wu, G. W. Peng, L. Liu, Y. P. Feng, Z. G. Huang, and Q. Y. Wu, Appl. Phys. Lett. **89**, 142501 (2006).
[24] C. Das Pemmaraju and S. Sanvito, Phys. Rev. Lett. **94**, 217205 (2005).
[25] I. S. Elfimov, S. Yunoki, and G. A. Sawatzky, Phys. Rev. Lett. **89**, 216403 (2002).